

Characteristics of Turbulent Nonpremixed Jet Flames in Different Gravity Levels

C. A. Idicheria, I. G. Boxx and N. T. Clemens*

Department of Aerospace Engineering and Engineering Mechanics,
The University of Texas at Austin
Austin TX 78712-1085

Abstract

An experimental study was performed with the aim of investigating the structure of transitional and turbulent nonpremixed jet flames under three different gravity conditions (1 g, 20 mg and 100 μ g). The low-g conditions were achieved by using the 1.25-second and 2.2-second drop towers at the University of Texas and NASA-GRC, respectively. The flames studied were piloted, nonpremixed, propane, ethylene and methane jet flames at source Reynolds number ranging from 2000 to 10500. The principal diagnostic employed was time-resolved imaging of the visible soot luminosity. The luminosity time-sequences were used to compute mean luminous flame lengths, RMS fluctuations, and to investigate large-scale structure evolution and flame tip dynamics by using volume rendering. The “buoyancy parameter”, ξ_L (as defined by Becker and Yamazaki, 1978), was determined to be a sufficient parameter for quantifying the effects of buoyancy on flame characteristics. The RMS fluctuations and volume renderings suggest that the large-scale structure and flame tip dynamics are essentially identical to those of purely momentum driven flames provided ξ_L is less than approximately 2-3.

Introduction

The work of Becker and Yamazaki [1,2] and Becker and Liang [3] were among the first to systematically study the effects of buoyancy on the characteristics of turbulent nonpremixed jet flames like soot formation, entrainment and flame length. They proposed that the effects of buoyancy could be quantified by a non-dimensional “buoyancy parameter”, ξ_L (defined below), which quantifies the relative importance of buoyancy at the flame tip location. They concluded that the effects of buoyancy on the characteristics of the flame become negligible when this non-dimensional parameter is less than unity. In their experiments, they lowered ξ_L by increasing the Reynolds number; however, this poses an important question as to whether any observed differences in the flame characteristics are an effect of the reduced effect of buoyancy or the increasing Reynolds number. Hence, it is not clear to what extent Becker and Yamazaki [1] were able to isolate the effects of buoyancy.

In the past couple of decades, the microgravity environment has been used to investigate the effects of buoyancy on a wide range of combustion systems. The microgravity environment offers the advantage of isolating buoyancy effects without simultaneous changes in the Reynolds number. Bahadori *et al.* [4] and Hegde *et al.* [5,6] were among the first to investigate nonpremixed jet flames in the laminar to turbulent regime in normal and microgravity conditions. Their results showed that there are significant differences in the characteristics of normal and microgravity nonpremixed jet flames. For example, at a Reynolds number of about 5000, their

microgravity flames were more than twice as long as their normal gravity flames, the latter of which had $\xi_L \approx 6.5$. This indicates a much stronger dependence of flame length on ξ_L than would be indicated by the results of Becker and Yamazaki [1]. Therefore, this raises the issue of whether ξ_L is a sufficient parameter for quantifying the effects of buoyancy.

Objectives

This work aims to investigate and clarify the role of the Reynolds number and ξ_L on buoyancy effects by obtaining qualitative and quantitative data for turbulent nonpremixed jet flames in different gravity levels. This work will also emphasize how buoyancy effects alter the turbulent structure of nonpremixed jet flames, in particular the characteristics such as flame length, luminosity fluctuations and structure celerity. This is achieved by studying nonpremixed jet flames at a range of Reynolds numbers and under three different gravity levels. The three gravity levels make it possible to alter the value of ξ_L through two orders of magnitude, while maintaining the same Reynolds number. The reduced gravity levels are achieved by using the 1.25-second University of Texas drop tower facility (UT-DTF) and 2.2-second drop tower at NASA-GRC. The primary diagnostic employed is high-speed luminosity imaging of turbulent nonpremixed jet flames.

Experimental apparatus

The low and microgravity experiments were conducted by dropping a self-contained drop-rig in two

* Corresponding author: clemens@mail.utexas.edu

different drop towers. The drop-rig was enclosed within a standard NASA-GRC 2.2-second drop tower frame. The drop-rig consisted of a turbulent jet flame facility and an onboard image and data acquisition system. The fuel jet issued from a 1.75 mm (inner diameter) stainless steel tube, with a 25.4 mm diameter concentric, premixed, methane-air flat-flame pilot. The pilot flame was used to ignite the main jet during the drop and also to keep the jet flame attached. Flame luminosity was imaged using a Pulnix TM-6710 progressive scan CCD camera, capable of operating at 235 fps or 350 fps at resolutions of 512×230 pixels and 512×146 pixels respectively. The camera was electronically shuttered, with the exposure time depending on flame luminosity (1/235 to 1/2000 seconds), and was fitted with a 6mm focal length, f/16 CCTV lens, chosen to maximize the field of view (typically 405mm). The drop-rig was fully automated through a custom configured onboard computer (CyberResearch Inc). A more detailed description of the drop-rig and the 1.25-second drop-tower is given in Refs. 7,8.

Experimental Conditions and Considerations

Three different jet fuels were studied (propane, ethylene and methane) and experiments were conducted for a range of Reynolds numbers ($2000 < Re_D < 10500$). The Reynolds number ($Re_D = U_o D / \nu$) is based on the jet exit diameter (D), jet exit velocity (U_o) and the kinematic viscosity (ν) of the fuel at room temperature. The “buoyancy parameter,” is defined as $\xi_L = Ri_s^{1/3} L / D_s$, where Ri_s is the source Richardson number ($Ri_s = g D_s / U_s^2$) based on the source diameter $D_s = D(\rho_o / \rho_\infty)^{1/2}$, and source velocity $U_s = U_o$ for a top-hat velocity profile round jet. L is the average visible flame length, g is the acceleration due to gravity, ρ_o is the jet fluid density and ρ_∞ is the ambient density. The experiments were conducted for three different gravity levels of 1 g, 20 mg and 100 μ g. Thus, for the different fuels studied ξ_L varied from 3.7 to 12.0 in normal gravity, 1.0 to 4.0 in milligravity and 0.22 to 0.66 in microgravity conditions.

The 2.2-second drop tower at NASA GRC provides microgravity levels of 100 μ g, and accelerometer measurements acquired in the UT-DTF indicate low gravity levels ranging from 10 mg at the beginning of the drop, rising to 30 mg by the end. Hence, the ξ_L values for the milligravity cases were computed at 20 mg. The relatively high g-levels in the UT tower were due to the fact that no drag shield was used. However, to reduce the effects of outside disturbances the sides of the drop-rig were closed with aluminum sheets.

Results and Discussion

The image time-sequences acquired during the drops reveal the start-up transient and the attainment of a stationary state. In both the 1.25-second and 2.2-second

towers, the startup transient was less than about 0.3 seconds (e.g. see Fig. 6). Mean and RMS luminosity images were computed from the time-sequences, excluding the startup and shutdown transient frames. Sample mean flame images for ethylene and propane at different Reynolds numbers and buoyancy parameters are presented in Fig 1. For comparison, sample instantaneous images, from which the means were computed, are shown in Fig. 2. The instantaneous images were sampled from the steady state portion of the flame time history. Each set of images separated by vertical lines (Fig. 1a-1d) is for the same fuel type and Reynolds number. All of the cases with $\xi_L < 1$ were taken in microgravity, cases with $1 < \xi_L < 3$ were taken in milligravity, and cases with $\xi_L > 3$ were taken in normal gravity. For example, Fig. 1a shows the mean luminosity images for ethylene at $Re_D = 10,500$ in normal and milligravity environments. This image pair shows that the $\xi_L = 3.7$ flame appears to be very similar to the $\xi_L = 1$ flame. A careful viewing of all of the images in Fig. 1 strongly suggests that flames with ξ_L near unity and below are essentially identical in their mean luminosity (flame height and width). Differences start to appear as the ξ_L values become farther apart as seen from Figs. 1b-1d.

Figure 3 shows the variation of the mean visible flame length (obtained from mean images) normalized by the tube exit diameter for all the cases studied. Sample precision uncertainty levels (95% confidence) computed from repeated runs are also shown. The confidence intervals are in the range of $\pm 4D$ to $\pm 35D$ for all three flames, with higher differences at the lower Reynolds number cases. It is evident from Fig. 3 that the flame lengths converge under different gravity levels with increasing Reynolds number for ethylene and propane. Only low Reynolds numbers are shown for methane because at higher Reynolds numbers, the flames were lifted, which we wanted to avoid. For the different Reynolds numbers of ethylene, the maximum variation in the mean flame length is $\pm 15\%$ ($Re_D = 2,500$ and $5,000$). For $Re_D = 2,500$ the normal-gravity flame is shorter than the milligravity and microgravity flames, whereas the trend is opposite for $Re_D = 5,000$. However in the higher Reynolds number cases, the variation in flame length is less than $\pm 10\%$. For propane, a significant difference is seen only in the lowest Reynolds number whereas in all the other cases the difference is less than $\pm 10\%$.

Figure 3 also shows the data of Hegde *et al.* [6] for propane flames under normal and microgravity. Their data and the present data differ substantially at Reynolds numbers less than 3000, although it appears that there is better agreement for the normal gravity case. Computing visible flame lengths will depend on the particular definition of the length, and therefore absolute differences are not surprising. However, they show a very large difference between normal and microgravity flames even

for Reynolds numbers greater than 4000. Note that similar differences between normal and microgravity flames were

observed for methane and propylene also [5].

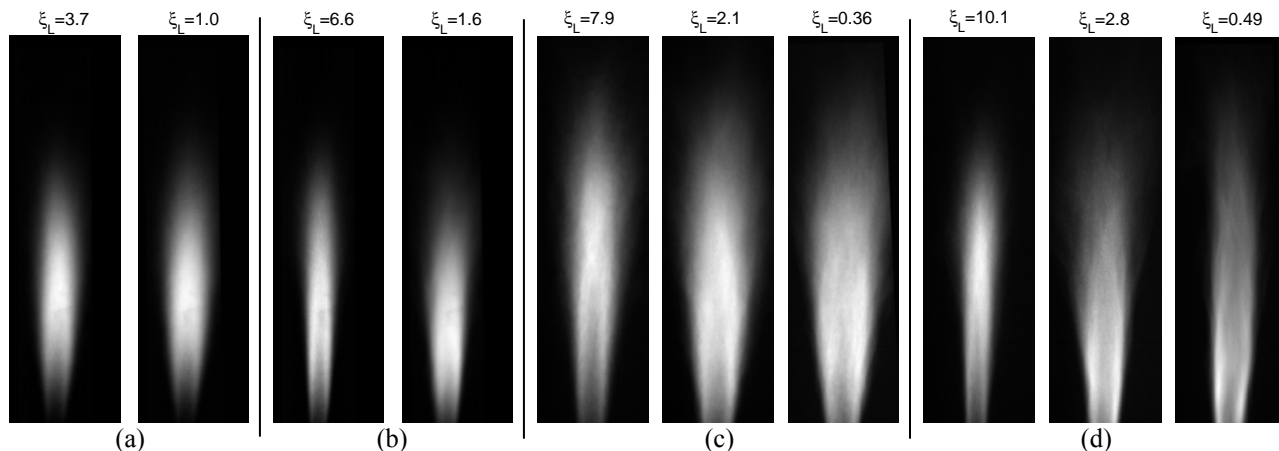


Figure 1: Sample mean luminosity images: (a) Ethylene $Re_D=10,500$, $43 < x/D < 279$, (b) Ethylene $Re_D=5000$, $43 < x/D < 279$, (c) Propane $Re_D=8500$, $76 < x/D < 308$, and (d) Propane $Re_D=5000$, $76 < x/D < 308$.

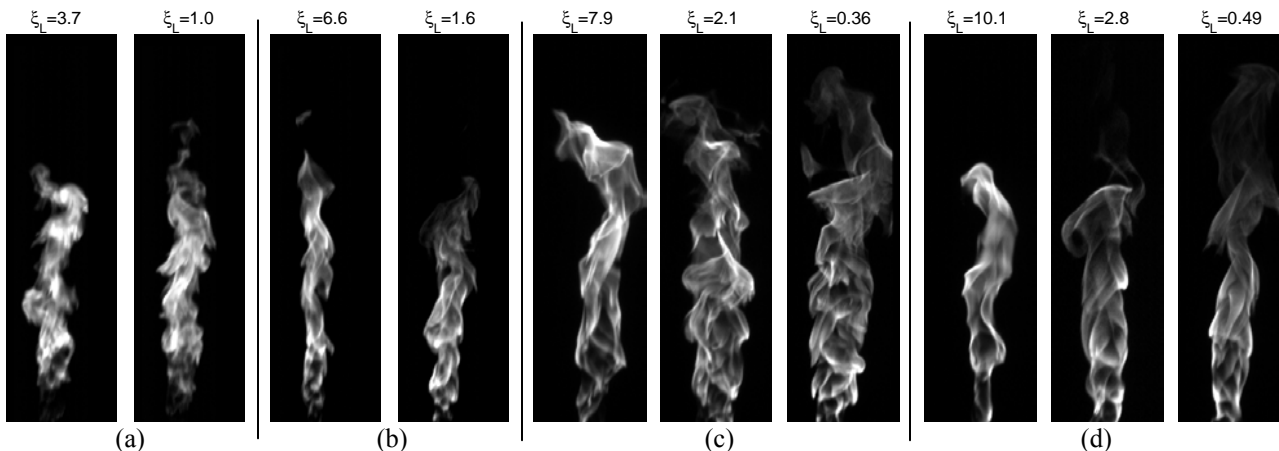


Figure 2: Sample instantaneous luminosity images: (a) Ethylene $Re_D=10,500$, $43 < x/D < 279$, (b) Ethylene $Re_D=5000$, $43 < x/D < 279$, (c) Propane $Re_D=8500$, $76 < x/D < 308$, and (d) Propane $Re_D=5000$, $76 < x/D < 308$.

A primary difference between these previous studies and the present is the presence of our pilot flame to keep the jet flame attached. If the flames in the previous studies were lifted in normal gravity, the flame length could be shorter (when compared to an attached normal gravity flame) and therefore if microgravity caused the flame to attach, then it is possible that the flame could become longer. We conducted tests at normal gravity to see if our non-piloted lifted propane flames differed substantially in their length from the piloted attached flames. The differences seen in the flame heights for these conditions were negligible and in some cases the lifted flame was longer than the piloted flame. Hence, we can argue that the large difference in flame length seen in previous studies is apparently not due to the presence of the pilot flame. The most obvious possibility for the difference between the normal and microgravity flames of Ref. 6 is

that differences in the levels of buoyancy as quantified by ξ_L are much larger than were tested in the present study. This is apparently not the case, however, as in Ref. 6, the $Re=5000$ flame has $\xi_L = 6.5$ and 0.5 , for the normal and microgravity flames, respectively. As Figs. 1c and 1d shows, we do not see such dramatic differences in flame length for differences in ξ_L of this magnitude. To assess the sensitivity of our flame length, we also tested our burner in various configurations. Specifically, normal gravity tests were conducted with the burner inside and outside the drop rig, with and without the pilot flame housing. In all these tests, the difference seen was small.

Another possible reason for the disagreement could be that transitional microgravity flames are much more sensitive to the boundary conditions, such as ambient disturbances, than normal gravity flames. It can be argued that the reason for this increased sensitivity is because

removing buoyancy effects removes a major source of disturbances that hasten the transition to turbulence. Thus removing this source of disturbances leaves the flame sensitive to other, possibly much weaker, disturbances. Therefore, slight differences in the flow configuration in the present work and Hegde *et al.* [5,6], such as differences in the enclosures, may lead to large differences in the flame height observed under low-gravity conditions.

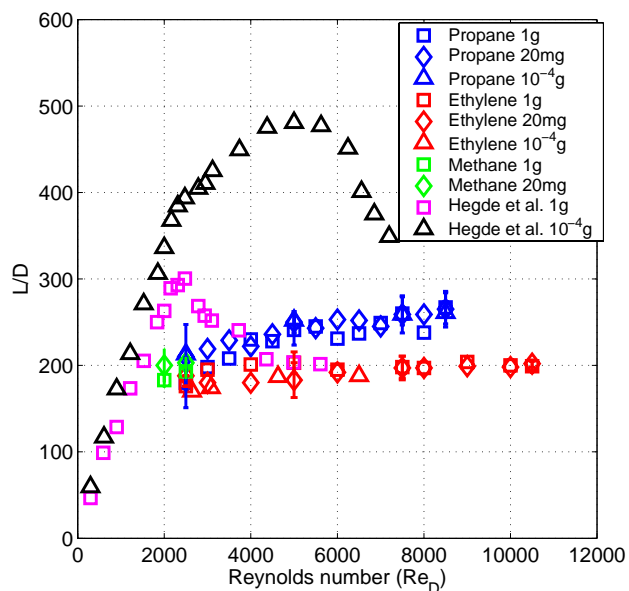


Figure 3: Variation of normalized flame length with Reynolds number at different gravity levels

Figure 4 shows a comparison between the present normal gravity flame length data to other published data. Specifically, it shows the present data plotted along with the data of Becker and Yamazaki [1] and Mungal *et al.* [9]. It can be seen that the present data agree quite well both in trend and in value to previously published work for the same fuel and the same range of Reynolds number.

The RMS fluctuations of the flame luminosity time-sequences were computed to determine if the trends that were observed in the mean images are also seen in fluctuating quantities. Soot luminosity cannot simply be related to any particular property of the soot, such as soot volume fraction. Furthermore, if the RMS fluctuations for two cases are different, it could be due to differences in either the soot properties or the underlying fluid mechanics. The RMS fluctuations are still useful to compute, however, because we are interested in potential differences, regardless of the underlying mechanism. Figure 5a shows RMS images for the ethylene flames at Re_D=10,500 in normal and low gravity. They have noticeable similarities, but clear differences are apparent such as the lower peak RMS values on the centerline of the $\xi_L=1.0$ flame. However, more drastic differences

arising due to effects of buoyancy can be seen when comparing flames with a larger difference in ξ_L (Fig. 5b). Figures 5c and 5d compare the RMS images of propane flames (Re_D=8,500 and 5,000). In Fig. 5c it is seen that the fluctuations are nearly identical for the $\xi_L=2.1$ and 0.38 cases, but both differ substantially from the $\xi_L=7.8$ case. A similar trend is observed for the image set of Fig. 5d. We can conclude then, that large fluctuations are present near the flame tip in the large ξ_L flames, which is expected since buoyancy acts on fluid volumes and so its effects are more prevalent near the flame tip where the large-scale vortical structures are formed. Interestingly, regardless of fuel type or Reynolds number, the low ξ_L flames all have qualitatively similar RMS contours: the fluctuations peak near the periphery of the flame and remain low even at the flame tip.

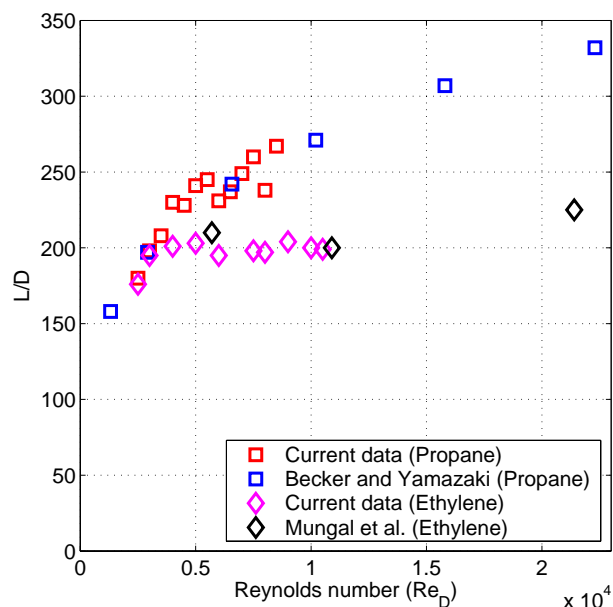


Figure 4: Comparison of current normal-gravity flame length data with other published data

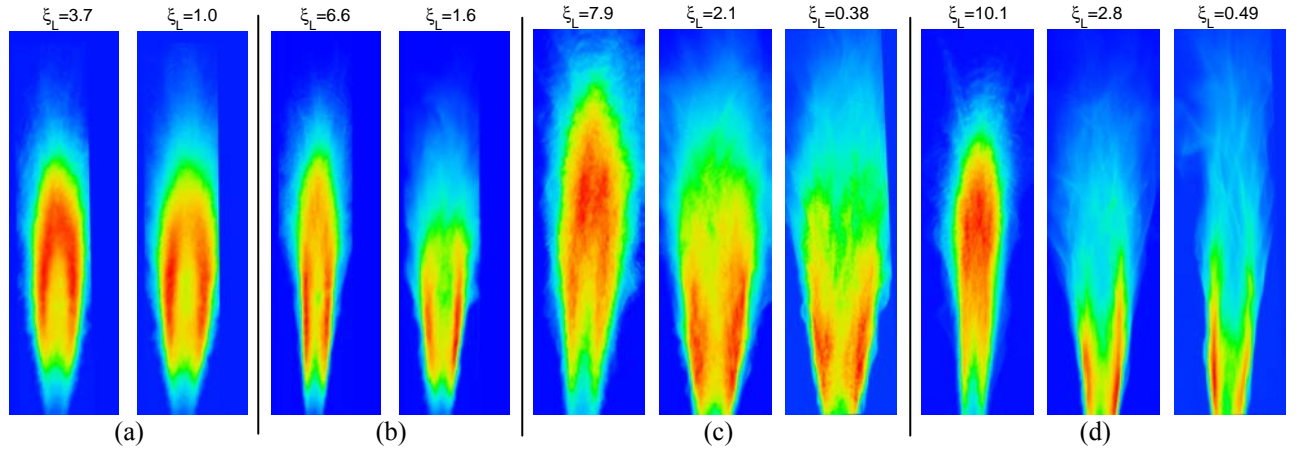


Figure 5: Sample RMS luminosity images: (a) Ethylene $Re_D=10,500$, $43 < x/D < 279$, (b) Ethylene $Re_D=5000$, $43 < x/D < 279$, (c) Propane $Re_D=8500$, $76 < x/D < 308$, and (d) Propane $Re_D=5000$, $76 < x/D < 308$.

The characteristics of the flame tip fluctuations are shown in Fig. 6. These data are for propane flames at varying Reynolds number, and were generated by computing the instantaneous luminous flame length from the instantaneous images. Because higher Reynolds number flames are achieved by increasing the jet exit velocity, the time axis has been scaled by the characteristic time scale, D/U_0 . Since the framing rate is not fast enough to detect small-scale fluctuations in the flame tip, we expect Reynolds number effects will not be very significant in these plots. These plots show that the flame tip fluctuations are very similar for values of ξ_L of 2.8 and below. The $\xi_L=7.9$ case seems to exhibit higher frequency fluctuations, and this is clearly the case at $\xi_L=10.1$. These higher-frequency fluctuations are due to the increased velocities caused by buoyant acceleration.

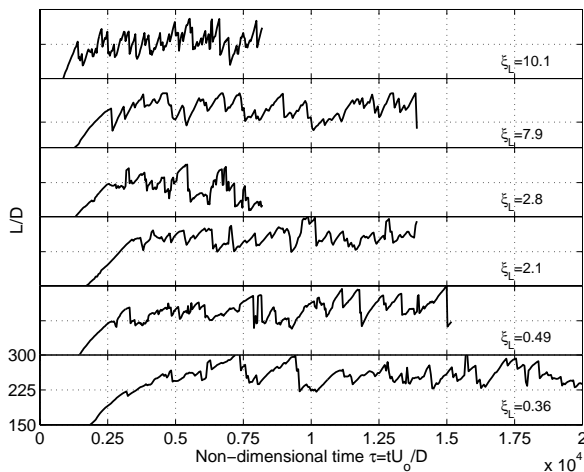


Figure 6: Instantaneous flame tip location for propane flames at various ξ_L .

Volume rendering of jet flame image sequences was used to investigate the large-scale structure characteristics. In this technique [9], 3-D isocontours

(x,y,t) of the jet flame edge are generated, allowing qualitative comparisons of such features as large-scale structure evolution and propagation velocities. The slope of each wrinkle in the 3-D iso-contour of the visible flame edge is proportional to the large-scale luminous structure propagation velocity (celerity). Using this technique, Mungal *et al.* [9] found the celerity to be $12 \pm 2\%$ of the jet exit velocity irrespective of the buoyancy parameter and fuel type (see Fig. 7). This is an intriguing result because the jet centerline velocity decays with downstream distance, but apparently not that of the luminous structures. In Ref. 9, it was suggested that the reason for this is that as a structure propagates farther downstream it moves towards the centerline (following the stoichiometric contour) where the velocity is higher. By continuously moving inward, the structure can maintain a constant velocity.

The actual renderings are not shown due to space constraints and can be seen in Refs. 7,8. Figure 7 shows the plot of the ratio of celerity to jet exit velocity, U_s/U_0 (%), against the buoyancy parameter, ξ_L . The normal gravity flames (high ξ_L values) are associated with higher celerity which can be attributed to the buoyant acceleration. This suggests that the more buoyant flames will have higher celerity and that it is in fact buoyancy dependent, contrary to the findings of Mungal *et al.* [9]. Since Mungal *et al.* [9] studied higher Reynolds number jet flames it is possible that the disagreement is due to a Reynolds number effect. As the ξ_L value decreases and is approximately less than 4, the celerity becomes independent of the gravity level and fuel type. In this regime, there is reasonable agreement with the findings of Mungal *et al.* [9].

Figure 8 shows the celerity values (normalized by jet exit velocity) plotted against Reynolds number for different gravity levels, where it is seen that the high celerity cases correspond to low Reynolds numbers. As

the Reynolds number increases the celerity decreases and becomes independent of the gravity level as can be seen in the case of ethylene. However, this trend is not readily visible for propane. This is to be expected since the highest Reynolds number case studied for propane has substantially different ξ_L values ($Re_D=8500$, $\xi_L=7.9$ at 1 g and $\xi_L=2.1$ at 20 mg).

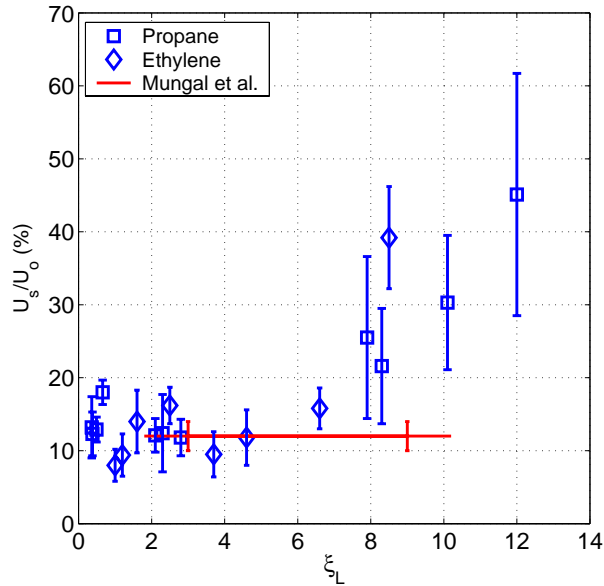


Figure 7: Normalized celerity of large-scale structures vs. ξ_L .

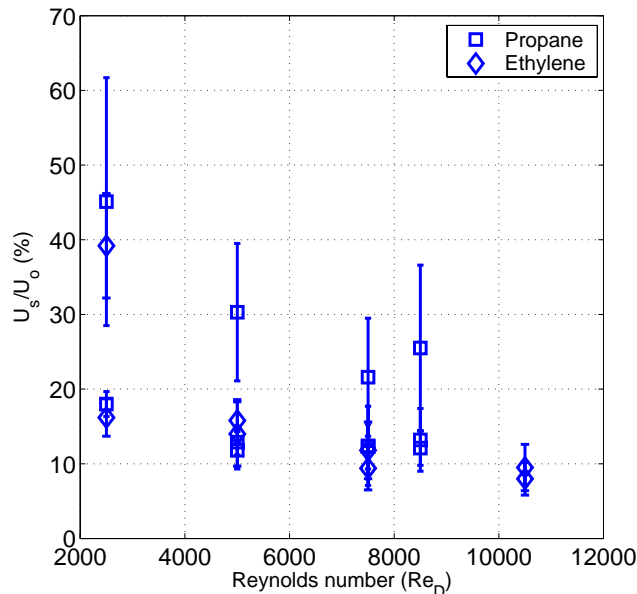


Figure 8: Normalized celerity of large-scale structures vs. Reynolds number.

Conclusions

The characteristics of turbulent nonpremixed jet flames were studied at Reynolds numbers ranging from

2,000 to 10,500 and at three levels of gravity: 1 g, 20 mg and 100 μ g. The flames were piloted with a small premixed methane-air flame to keep it attached to the flame base for all Reynolds numbers considered. Time-resolved imaging of the natural soot luminosity was used to investigate the mean and RMS luminosity, flame tip dynamics, and evolution of large-scale structures using volume rendering. It was found that the Becker and Yamazaki buoyancy parameter, ξ_L , is sufficient to quantify the effects of buoyancy on both the mean luminosity and different measures of the fluctuations, provided the flame is turbulent. Our results suggest that the structure of the large-scale turbulence reaches its momentum-driven asymptotic state for values of ξ_L less than about 2-3. The large-scale luminous structure propagation velocity obtained from the volume renderings was also found to depend both on ξ_L and Reynolds number. The large differences in flame lengths for normal and microgravity flames previously reported in the literature were not found in this study.

Acknowledgments

This research is supported under co-operative agreement NCC3-667 from the NASA Microgravity Sciences Division with Dr. Zeng-guang Yuan of NCMR as technical monitor. We would also like to acknowledge useful discussions with Dr. Uday Hegde regarding the effects of boundary conditions on microgravity flames.

References

1. Becker, H. A. and Yamazaki, S., *Combust. Flame* 33: 123-149 (1978).
2. Becker, H. A. and Yamazaki, S., *Proc. Combust. Inst.* 16:681-691 (1977).
3. Becker, H. A. and Liang, D., *Combust. Flame* 32: 115-137 (1978).
4. Bahadori, M.Y., Stocker, D.P., Vaughan, D.F., Zhou, L. and Edelman, R.B., in *Modern Developments in Energy, Combustion and Spectroscopy*, Pergamon Press, 1995, pp. 49-66.
5. Hegde, U., Zhou, L., Bahadori, M. Y., *Combust. Sci. Technol.* 102:95-100 (1994).
6. Hegde, U., Yuan, Z.G., Stocker, D.P. and Bahadori, M.Y., *Proc. of Fifth International Microgravity Combustion Workshop*, pp. 259-262 (1999).
7. Idicheria, C.A., Boxx, I.G. and Clemens, N.T., AIAA paper 2001-0628 (2001).
8. Clemens, N.T., Idicheria, C.A. and Boxx, I.G., *Proc. of Sixth International Microgravity Combustion Workshop*, pp. 133-136 (2001).
9. Mungal, M.G., Karasso, P.S. and Lozano, A., *Combust. Sci. Technol.* 76:165-185 (1991).